

Manuscript Number: POWTEC-D-20-00392R1

Title: Variation in particle size fraction to optimize metal injection molding of water atomized 17-4PH stainless steel feedstocks

Article Type: Research Paper

Keywords: particle size fraction; sphericity; dimensional tolerance; metal injection molding

Corresponding Author: Professor Berenika Hausnerova, prof

Corresponding Author's Institution: Centre of Polymer Systems

First Author: Bhimasena N Mukund

Order of Authors: Bhimasena N Mukund; Berenika Hausnerova, prof

Abstract: This work reports on an essential effect of rather slight size differences in water atomized 17-4PH stainless steel powder on resulting microstructure and dimensional tolerances of metal injection molding (MIM) parts. The powders of round to irregular shapes prepared in three different powder volume fractions were admixed into the paraffin wax/HDPE (50/50) binder in a double sigma mixer. After determination of critical solid loading, the rheological, molding, and sintering performance of 66 vol. % solid loading feedstocks was tested on complex-shaped MIM component. The slight differences in size fractions are reflected also in the powder shape, which was quantified through sphericity factor and aspect ratio by dynamic image analysis. The results indicate an increase in viscosity, flow instability and injection pressure, lower sintered density with enhanced dimensional deformations for feedstocks having higher amount of coarser (10-20) μm fraction accompanied with higher shape irregularity determined from sphericity factor and aspect ratio.

Editor, Powder Technology
April 16, 2020

Dear Sir

Enclosed please find the revised manuscript entitled

"Variation in particle size fraction to optimize metal injection molding of water atomized 17-4PH stainless steel feedstocks".

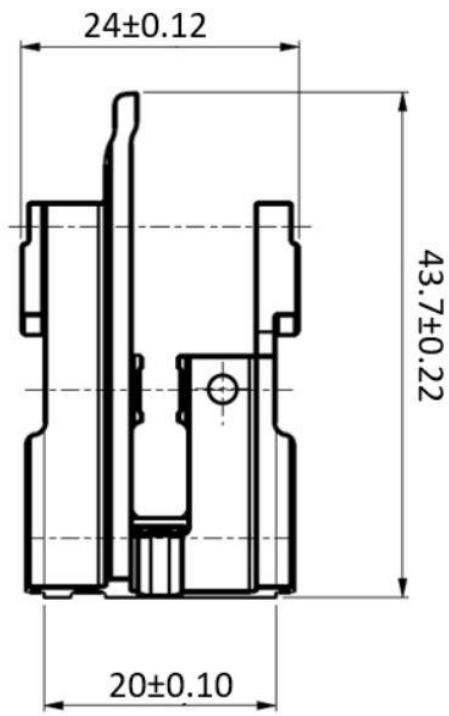
This paper reports on the effect of tailoring of particle size distribution of water atomized stainless steel powder on the performance of a complex-shaped part produced with metal injection molding. It shows that only a slight variation in the particle size fractions considerably influences the processability and resulting dimensional tolerances of sintered parts.

The article is original, unpublished and is not being considered for publication elsewhere. I would highly appreciate if you would consider the possibility to publish this work in your journal Powder Technology.

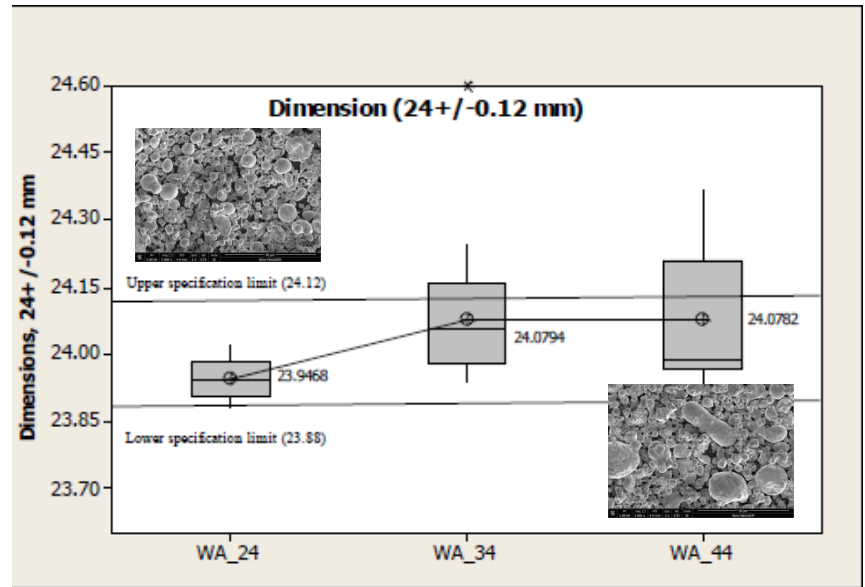
Sincerely yours,

A handwritten signature in black ink, appearing to read 'Berenika Hausnerova', with a stylized, flowing script.

Berenika Hausnerova



Powder size and sphericity tailoring to MIM tolerances



*Highlights (for review)

- 17-4 PH MIM feedstocks tailored to three different powder volume fractions
- powder shape quantified using dynamic image analyzer
- injection molding parameters optimized for complex-shaped item
- variation in coarse size fraction influences flow stability of feedstocks
- variation in coarse size fraction considerably affects dimensional tolerances

ABSTRACT

This work reports on an essential effect of rather slight size differences in water atomized 17-4PH stainless steel powder on resulting microstructure and dimensional tolerances of metal injection molding (MIM) parts. The powders of round to irregular shapes prepared in three different powder volume fractions were admixed into the paraffin wax/HDPE (50/50) binder in a double sigma mixer. After determination of critical solid loading, the rheological, molding, and sintering performance of 66 vol. % solid loading feedstocks was tested on a complex-shaped MIM component. The slight differences in size fractions are reflected also in the powder shape, which was quantified through sphericity factor and aspect ratio by dynamic image analysis. The results indicate an increase in viscosity, flow instability and injection pressure, lower sintered density with enhanced dimensional deformations for feedstocks having higher amount of coarser (10-20) μm fraction accompanied with higher shape irregularity determined from sphericity factor and aspect ratio.

The manuscript has been corrected according to the valuable comments (both fundamental and formal) of the Reviewers. We appreciate their effort and time spent to help us.

Reviewer #1: This paper investigates the effect of powder size differences and the corresponding shape differences on key parameter for MIM. The paper is well written, and the design of the experiment and the results and discussion are clear. I would recommend it for publication with several minor changes being made.

1. There are no captions for all the figures and tables. – *included in the revised version*

2. The SEM micrographs of powders (Fig. 2, examples for WA_24 and WA_44) indicate round to irregular shaped particles. Do the authors mean round for WA_24 and irregular for WA_44? Or for each of them, there are both round and irregular ones? I understand the latter is true but it is important to clarify this so that readers can better understand the following discussion. – *yes, the latter is correct, we tried to express it clearly in the revised manuscript in order not to confuse the readers*

3. Section 3.2: The authors identify several trends of CSL, Sw and n among WA_24, WA_34 and WA_44, and discuss the relationship of these trends. How do the authors determine if these trends are CLEAR? I mean, for example, the difference between Sw for WA_34 and Sw for WA_44 is less than 2%, and the CSL for those three compounds are 71, 70 and 69%. How do the authors determine if these differences are significant or insignificant? – *yes, you are right, the differences are rather small, and we had to be really careful to intercept them. Slight differences are attributed to the slight differences in the PSD (and as a consequence also shape) of the tested feedstocks. However, this is exactly the point – only little difference in the powder characteristic resulting in the slight variation of important parameters as CSL has the essential effect on the resulting MIM parts performance; in fact, the small powder characteristics variation decides if the part meets the tolerances or not. Thank you for matching this point – we stress it in the revised abstract as well.*

4. Section 3.3: This is attributed to the flow performance and structure stability associated with the higher coarser particle fraction (WA_44). It would be better to clearly describe what the flow performance and structure stability of WA_44 are, in order to make the argument more convincing. – *according to our long term research in MIM we feel more and more stronger that the stability of the viscosity, i.e. its repeatability and independence on time, is more important variable than its variation with the shear rate. However, in present, almost all research published (including our own papers) relays on the dependence of viscosity on shear rate, and reports flow index to be the key parameter for successful injection molding. We modified the text as highlighted.*

5. Fig. 7: (1) Keep all the format for the two figures same. – *done in the revised version*

(2) which can be also attributed to the coarser particle fractions with the lower sphericity: I'm confused which one is more important, size, shape or both? It would be good to describe it more clearly. – *in general, both: in our previous paper we found out that for coarse (11 and 20 μm) particles, the processability is better in the case of spherical (gas atomized powders), whereas in the*

case of fine powders (3 and 8 μm), water atomized feedstocks show a better performance. The latter is rather opposite to generally accepted statements concerning the effect of particle shape on flow behavior of filled polymer melts. I am afraid it is too early to say, which one is dominant, as we have still not enough reliable data to make generally applicable rule, and the data which can be found in the literature does not help much in this respect as well.

6. A general concern is that while the title of this paper mentions the particle size fraction only, both size and shape affect the quality of MIM components. I'm glad that the authors already clearly say this point in the abstract and conclusion. It would be good to emphasize this point when discussing the dependence of viscosity, flow instability and other parameters on these two factors. – *to distinguish the effect of shape and size is a tricky task, we addressed that in the previous paper published (Powder Technol. 312, 2017), where we had a unique possibility to work with a set of 4 powders produced by GA and 4 powders produced by WA, with PSD always kept similar for one GA and WA “couple”. The main result of this study is that in order to satisfactorily distinguish between the effects of shape and size not only more data, but another type of modelling must be employed. At the moment we are working on the project producing so called master curves to help to find an answer.*

Reviewer #2: The present work is very interesting and consequently extends the existing knowledge in metal injection molding. The manuscript is well structured and very clearly written.

Minor comments:

* Caption of section 3.1: ... characteristics - *corrected*

* Quality of figure 6 should be improved, some magnifications for a certain region would be helpful, and the quality of the reference length have to be improved since it is not readable – *improved*
- *thank you for your kind evaluation and comments, which are reflected in the revised version of the paper*

Variation in particle size fraction to optimize metal injection molding of water atomized 17-4PH stainless steel feedstocks

Bhimasena Nagaraj Mukund^{1,2} and Berenika Hausnerova^{1,3*}

¹Department of Production Engineering, Faculty of Technology, Tomas Bata University in Zlin, nam. T.G. Masaryka 5555, 760 01 Zlin, Czech Republic

²Indo MIM Pvt. Ltd., KIADB Industrial Area, Hoskote, Bangalore 562114, India

³Centre of Polymer Systems, University Institute, Tomas Bata University in Zlin, Nad Ovcirnou 3685, 760 01 Zlin, Czech Republic

*Corresponding Author; Phone: +420 57 603 5167, E-mail: hausnerova@utb.cz

ABSTRACT

This work reports on an essential effect of rather slight size differences in water atomized 17-4PH stainless steel powder on resulting microstructure and dimensional tolerances of metal injection molding (MIM) parts. The powders of round to irregular shapes prepared in three different powder volume fractions were admixed into the paraffin wax/HDPE (50/50) binder in a double sigma mixer. After determination of critical solid loading, the rheological, molding, and sintering performance of 66 vol. % solid loading feedstocks was tested on a complex-shaped MIM component. The slight differences in size fractions are reflected also in the powder shape, which was quantified through sphericity factor and aspect ratio by dynamic image analysis. The results indicate an increase in viscosity, flow instability and injection pressure, lower sintered density with enhanced dimensional deformations for feedstocks having higher amount of coarser (10-20) μm fraction accompanied with higher shape irregularity determined from sphericity factor and aspect ratio.

Keywords: particle size fraction; sphericity; dimensional tolerance; metal injection molding

Introduction

Metal Injection Molding (MIM) technology inherits the advantages of plastic injection molding and powder metallurgy for manufacturing small-to-medium size precise metal components from different alloying composition such as steels (Fe2Ni, Fe7Ni, FeCr), stainless steels (SS 17-4PH, SS 420, SS 316L), high temperature alloys (HK30, Inconel 713) and high wear resistance alloys (cemented carbides). In general, any alloy available in a powder size ranging between 0.5 and 20 μm should be processable with MIM.

Technology involves consequent processing steps starting from identifying suitable powder and binder system for successful mixing and injection molding. Molded (*green*) components then undergo debinding, where a binder is removed through solvent, thermal or catalytic approach. After a complete binder removal, metal particles are sintered to form a dense structure of a metal body with density and mechanical properties similar to a wrought metal.

Selection of suitable powder type plays a key role in MIM, governing molding and sintering conditions. Gas atomized powders can be packed to high densities with suitable viscosity during injection molding, whereas their spherical shape limits the component strength during debinding and sintering [1-2]. However, lower oxygen in the gas atomized powders with enhanced powder packing results in a higher densification during sintering. In contrast, rounded or irregularly shaped water atomized powders exhibit higher resistance to flow and lower packing density due to the presence of oxides inducing porosity, and thus lower sintered density [3-6]. A comparison study of the 14 μm gas and water atomized powders after sintering in a hydrogen atmosphere at 1300 °C resulted in the sintered density of 98.9 % with the tensile strength of 1280 MPa for the spherically shaped powder, and 97.2 % with the tensile strength of 1080 MPa for the irregularly shaped one [7]. However, the difference in the obtained strength may be to some extent

eliminated by sintering of water atomized powder at higher temperatures. Often, the cost effective mixtures of gas and water atomized powders are used to improve the interparticle friction to resist the slumping during debinding [7,8].

Claudel *et al.* [9] investigated the effect of particle size distribution (PSD) of Inconel 718 feedstock on the rheological properties. The results indicate that lower the average particle size is, higher the critical solid loading can be achieved. The similar study on 316L feedstock by Sotomayor *et al.* [10] reports the increase in feedstock viscosity for finer size fractions in the powder. Further, shear sensitivity was found to decrease with particle size, whereas activation energy remained unchanged. Seerane *et al.* [11] studied the influence of PSD on the SS 17-4PH sintered parts and found out that the coarser PSD (12-50 μm) yielded minimum shrinkage and inferior sintered density, whereas fine PSD (2-8 μm) resulted in higher shrinkage, lower sintered densities due to agglomerations, but superior mechanical properties. A study provided on four gas atomized Inconel 718 powders ranging from fine (<22 μm) to coarser fractions (65-212 μm) by Contreras *et al.* [12] stresses the advantages of broad PSD in terms of better packing and lower viscosity.

Regardless of a considerable research attention to demonstrate the influence of the powder characteristics as particle size distribution (PSD), mean size and shape, majority of them lack the possibility to distinguish between the effect of the shape and the size. In our recent work [13], this issue was considered and investigated for the set of gas (spherical) and water (irregular) atomized powders having the same mean sizes. It was found out that for coarse particles the processability in terms of rheological behavior is better in case of gas atomized powders in accordance with previous findings, but in case of fine powders, water atomized powders showed higher performance.

Also, the research has been so far focused mainly on advantages/disadvantages of finer and coarser particle size on a flow performance of feedstocks, and there are only rare papers [e.g. 4,5] devoted to optimize overall MIM process to obtain desirable mechanical performance and dimensional tolerances. Thus, in this work the emphasis is given to tailor particle size fractions to produce a defect free complex-shaped MIM parts from water atomized 17-4PH stainless steel powder.

2 EXPERIMENTAL

2.1 Materials and their characterization

Stainless Steel (SS) 17-4PH is a ferrous alloy containing (12 – 17) wt.% chromium, (4 – 8) wt.% nickel, and (0 – 4) wt.% copper with possible maximum additions of molybdenum (0.5 wt. %), silicon (1 wt. %), manganese (1 wt.%), and niobium (0.4 wt.%) and carbon (0.07 wt.%). Three different tailor-made particle size fractions were chosen for the feedstocks' preparation. Table 1 summarizes their key properties such as particle size distribution (PSD), pycnometer density (ρ_{pycn}), tap density (ρ_{tap}), and particle size distribution width (S_w). Malvern Master Sizer 3000, Hydro EV was used to measure D_{10} , D_{50} , D_{90} depicting the particle size of the powder at 10, 50 and 90 %, respectively, on a cumulative particle size distribution curve. The powder abbreviations (WA_24, WA_34 and WA_44) reflect the percentage of particles with the size between 10 μm to 20 μm obtained from water atomization.

Gas pycnometer (Accupyc 1330, Micromeritics) was used for determination of ρ_{pycn} of powders. The true volume of the solid was calculated from the drop in the pressure when the defined amount of gas (helium) was allowed to expand into the chamber containing the sample. Thus, the volume obtained with the pycnometer excludes the volume of pores. Tap density of

powders was determined according to MPIF 46. The defined mass of the powder was mechanically tapped until packed to the minimum volume, and the difference between before- and after-tapping was recorded [1].

Morphology of the powders was examined with a scanning electron microscope (NanoSEM 450, FEI) and a dynamic imaging analysis (Camsizer X2, Retsch Technology). The dynamic imaging analysis allows to measure quantitative particle shape parameters (ratio of round to irregular particles, satellites, agglomerates). The analyzer was equipped with two digital cameras with > 4 mega pixel resolution.

Wax-polymer binder system composed of 50/50 mixture of paraffin wax (PW, Polyaid G101, Gujarath Waxes, density 0.91 g.cm^{-3}) and high density polyethylene (HDPE, H2105, Huntsman, density 0.96 g.cm^{-3}) was utilized through this study (and our previous research of the effect of particle shape [13]), because there are no pronounced interactions complicating the study of the particular effect of powder size/shape as in the case of binders containing polar components as PEG and semicrystalline waxes [14,15].

2.2 Feedstock preparation

Haake PolyLab torque driven laboratory mixer was used to prepare the feedstocks. The mixer has the maximum capacity (chamber volume) of 69 cm^3 with in-built thermocouples to monitor a melt temperature during mixing. Roller rotors were used to mix the powder into the binder with 80 % of the chamber volume at $180 \text{ }^\circ\text{C}$. Mixer speed was set to 40 rpm and the feedstock response was recorded via the torque development with time. The binder ingredients were premixed for 10 minutes, followed by the addition of the powder into the mixing chamber.

2.3 Rheological properties

In order to study the effect of the particle size fractions on the rheological properties such as viscosity (η) and power-law index (n) a single bore capillary rheometer (SR20, Instron) with L/D ratio of 10/1 was used. Shear rates ranging from 500 to 10,000 s^{-1} were applied at 160, 170 and 180 °C. Time dependent viscosity measurement at a constant shear rate of 1000 s^{-1} and temperature of 180 °C was performed to interpret flow instabilities occurring in the feedstocks.

2.4 Injection molding

The MIM component tested has a mass of 25 g with length of 43.7 mm and complex design features such as multiple holes, slots and perpendicular features varying in cross-sections (Fig. 1). The components were molded in a CNC controlled Wittmann Battenfeld injection molding machine. The reciprocating screw with a diameter of 30 mm was used with a clamping force of 45 tons. Injection molding parameters such as barrel and nozzle temperatures, holding pressure, injection speed and switch over point were optimized for each feedstock prior molding green components on a large scale. Defects (if any) generated during injection molding were screened and related to the particle size fractions tested.

2.5 Debinding, sintering and heat treatment conditions

The binder was removed from the green parts through a combination of solvent and thermal debinding. The solvent debinding was performed by immersion of the green components in trichloroethylene at 50 °C for 300 min. The weight loss of the extracted binder component (paraffin wax) was controlled to reach the minimum of 90 % before moving forward to thermal debinding and sintering. The thermal debinding and sintering were performed inside a vacuum furnace by heating the components up to 600 °C followed by ramping up to 1350 °C in a partial

pressure under argon atmosphere. The sintered components continued for a solutionisation (1038 °C for 30 min) followed by heat treatment to H900 conditions (480 °C, 60 minutes). Metallurgical properties were investigated on the final, heat-treated samples. Microstructure of the heat-treated components was evaluated in a microscope (Nikon, Model Eclipse MA200) and density was determined using Archimedes principle.

3 Results and discussion

3.1 Evaluation of powder characteristics

The mean particle size (D_{50}) of the chosen water atomized powders is in the range of (8-9) μm (Table 1). Table 2 shows the tailored particle size distribution from fine (lower than 5 μm) fraction to coarse one (up to 35 μm). It is observed that the WA_24, WA_34 and WA_44 powders have the (10-20 μm) particle size fraction (highlighted in bold in Table 2) corresponding to 24, 34 and 44 %, respectively, while the coarsest volume fraction (20 - 35 μm) is kept similar. The SEM micrographs of powders (Fig. 2, examples for WA_24 and WA_44) indicate round to irregular shape of the tested powders resulting from the water atomization fabrication route.

As can be seen from Fig.2, the differences in size fractions are reflected also in the powder shape. Therefore, in order to describe the powder shape in a quantitative way, the most sensitive shape parameters – sphericity factor and aspect ratio – of the powders were measured with dynamic image analysis. The aspect ratio, defined as the ratio of the width to the length of the particle, attains a value between 0 (irregular) and 1 (spherical). Similarly ranging is the sphericity factor S_p , which describes the roundness of the particles:

$$S_p = 4\pi A / P^2 \quad (1)$$

where A is the particle area and P is its perimeter.

The WA_24 powder contains almost 58 % of spherical particles with sphericity index of 0.91, whereas WA_34 and WA_44 contain 52 and 41 % of spherical particles with sphericities of 0.89 and 0.87, respectively. Concerning aspect ratio, WA_24 powder reaches the value of 0.82, whereas WA_34 and WA_44 have aspect ratios of 0.8 and 0.76, respectively. Thus, the finer powder (WA_24) contains more particles having closer-to-spherical shape than the other two (WA_34 and WA_44).

3.2 Mixing and flow performance

The critical solid loading (CSL) of feedstocks was determined with the help of torque measurement as recommended e.g. in [16] and described in detail in our previous work [13]. CSL determined from torque measurement reveals the values 71, 70 and 69 vol.% for WA_24, WA_34 and WA_44 feedstocks, respectively. The CSL values agree with findings of Claudel *et al.* [9] as well as with the particle size distribution width S_w calculated from the cumulative size distributions of powders tested (Table 1). The lowest value of S_w reflecting the broad particle distribution is obtained for WA_24 feedstock, which in turn means the highest value of the critical (maximum) loading.

Figure 3, representing the mixing torque vs. time of the feedstocks having 66 vol.% solid loading, indicates homogeneous mixing of all three materials tested. Different values of the obtained stable torque are attributed to the differences in CSL . The higher shape irregularity in the WA_44 feedstock seems to enhance interparticle friction among the particles [1] exhibiting slightly higher fluctuations in the torque development with time.

Stability of a viscosity in time dictates an ability of a feedstock to sustain high shearing during molding. Any increase or fluctuation in the viscosity with time might indicate material

restructuralization induced by a flow. The stable and repeatable viscosity trends of WA_24 and WA_34 feedstocks considerably differ for the feedstock containing WA_44 powder (Fig. 4) indicating inhomogeneous distribution of the powder in the binder [17-19]. Higher shape irregularity in the WA_44 restricts the flow of the binder into the particle interstices, and thus induces the non-uniform distribution of the binder in the feedstock. Hence, the feedstock containing WA_44 failed to provide repeatable stability test results, which consequently might be a source of a failure of tolerances in the final products.

Figure 5 shows viscosity as a function of shear rate of the WA_24, WA_34 and WA_44 feedstocks at a temperature of 180 °C. All feedstocks exhibit pseudoplastic behavior with viscosity decreasing with shear rate. Power law index n reveals the deviation from Newtonian flow behavior; lower the n value, stronger the shear rate dependency of viscosity is. The n values obtained for the tested feedstocks are: 0.40, 0.44 and 0.46 for WA_24, WA_34 and WA_44, respectively, reflecting molecular chain ordering of the binder and the particle orientation in the flow direction [2, 10, 20]. In this respect, particles in the WA_24 feedstock tend to orientate more easily with the flow than WA_34 and WA_44 feedstocks.

It should be noted that overall low viscosity values obtained for the tested feedstocks can be influenced by their slip at a capillary wall during measurement and/or the yield stress, which is typical phenomenon for particle compounds [21].

3.3 Injection molding

Molding parameters largely depend on powder characteristics, binder formulation, and feedstock homogeneity. Crucial molding parameters in injection molding include melt and mold temperatures, injection speed, holding pressure and time, switch over time and cooling time [22].

The optimized molding parameters adopted during injection molding of the complex-shaped

MIM component (see Fig.1) are presented in Table 3. The temperature of the feedstocks in the barrel was maintained between 170-180 °C to fill the cavity of the mold. The feedstock containing WA_24 powder filled the cavity easily at the nozzle temperature of 180 °C, whereas WA_44 compound was found to have the short fill in the molded component at the same temperature due to the fact that the WA_44 feedstock exhibits more resistance towards flow, which is detrimental for the successful injection molding of the complex geometry [1,20]. Hence, the nozzle temperature was gradually increased from 180 °C to 195 °C to completely fill the components with WA_44 compound. Apart from the nozzle temperature, other parameters as the barrel temperature, holding pressure and time, injection speed and switch over point (SOP) were kept constant for all feedstocks. The initial metering stroke was maintained to 42 cm³ and the injection screw was moved till the SOP up to 32 cm³ to fill approximately 10 cm³ of the molten material into the cavity of the mold. Filling percentages of the MIM component were 60, 52 and 49 % for WA_24, WA_34 and WA_44, respectively, in the filling phase, whereas the rest of the component was successfully filled completely in the packing phase. The changeover injection pressure generated during molding was found to be significantly higher (897 bar) for WA_44 feedstock compared to 623 and 758 bar generated for WA_24 and WA_34, respectively. This is attributed to the flow performance of the feedstock containing the higher coarser particle fraction (WA_44), which is neither repeatable nor stable in time, reflecting a structure variation upon shearing. It seems that the stability of the viscosity, i.e. its time dependence, is more important variable than its variation with shear rate. Also, the green components produced using the feedstock containing WA_44 had rather rough surface compared to other two feedstocks.

3.4 Sintering and heat treatment

Molded components were debound by solvent and thermal route followed by sintering and heat treatment at H900 conditions to manufacture sintered components. All parts resulting from the WA_24, WA_34 and WA_44 feedstocks had no surface defects after sintering and HT in a vacuum furnace. The metallurgical properties of the final heat-treated metal components are depicted in Table 4. Any significant differences in densities and carbon contents were observed for as-sintered conditions and H900 treatment conditions. The lowest density of WA_44 samples might indicate feedstock inhomogeneity (revealed from the flow stability test). The hardness of the sintered parts in the range of 28-32 HRC shows insignificant differences among the powder particle fraction chosen. The same applies for the values of the hardness obtained after H900 treatment (37-41 HRC) indicating only very slightly noticeable effect of the variation in the powder particle fractions. The final microstructures presented in Fig. 6 show a fine martensitic structure of the produced 17-4PH material.

3.5 Dimensional stability

Complex-shaped MIM component had the critical slot dimensions as depicted in Figure 1. The effect of the powder particle fraction (WA_24, WA_34 and WA_44) on the extent of deformation was studied by considering two critical dimensions on the component, which govern the extent of the overall deformation. They involve the slot width of (24 ± 0.12) mm at the front and (20 ± 0.10) mm at the back. In general, an achievable tolerance in MIM is about 1 % of any basic dimension [1]. All the components were staged with the constant staging method. The variation in the dimensions would arise from the variation in the cross section, in-molded stresses, sintering stresses or volumetric shrinkage. As can be seen from Figure 7, WA_24 feedstock reveals dimensions within MIM tolerances, while components produced from WA_34 and WA_44 have standard deviations in dimensional variation up to 0.14 mm and 0.16 mm for

the dimension (24 ± 0.12) mm, respectively, which can be also attributed to the coarser particle fractions with the lower sphericity.

CONCLUSION

The results obtained within this study indicate that it is desirable to control and tailor the powder characteristics in terms of particular size fractions and as well as its shape in order to produce quality MIM components. The critical parameters include the particle size distribution and sphericity/aspect ratio of powder, stability of viscosity, injection molding parameters, and sintering deformation. The increase in the population of coarser particle fraction accompanied with relatively more irregular shape significantly influenced the quality of the green components and deformation tolerances in the mass production of the complex-shaped MIM component.

Acknowledgement

This work was performed with the financial support of the Ministry of Education, Youth and Sports of the Czech Republic – Program NPU I (LO1504).

REFERENCES

- [1] R.M. German, A. Bose, Injection Molding of Metals and Ceramics, second ed., Metal Powder Industries Federation, Princeton, 1997.
- [2] S. Park, Y. Wu, D.F. Heaney, X. Zou, G. Gai, R.M. German, Rheological and thermal debinding behaviors in titanium powder injection molding, *Met. Mater. Trans. A* 40 (2009) 215-222. <https://doi.org/10.1007/s11661-008-9690-3>.
- [3] R.P. Koseski, P. Suri, N.B. Earhardt, R.M. German, Microstructure evaluation of injection molded gas and water atomized 316 stainless steel powder during sintering, *Mater. Sci. Eng. A* 390 (2005) 171-177. <https://doi.org/10.1016/j.msea.2004.08.002>.

- [4] H.O. Gulsoy, N. Gulsoy, R. Calisici, Particle morphology influence on mechanical and biocompatibility properties of injection molded Ti alloy powder, *Biomed. Mater. Eng.* 24 (2014) 1861-1873. <https://doi.org/10.3233/BME-140996>.
- [5] H.O. Gulsoy, S. Ozbek, T. Baykara, Microstructural and mechanical properties of injection molded gas and water atomized 17-4 PH stainless steel powder, *Powder Metall.* 50 (2007) 120-126. <https://doi.org/10.1179/174329007X153288>.
- [6] D.F. Heany, R. Zauner, C. Binet, K. Cowan, J. Piemme, Variability of powder characteristics and their effect on dimensional variability of powder injection molded components, *Powder Metall.* 47 (2004) 144-149. <https://doi.org/10.1179/003258904225015491>.
- [7] P.K. Minuth, P. Kunert, D. Meinhardt, G. Venl, L. Kramer, T. Hartwig, Mechanical properties of MIM parts produced from mixtures of stainless steel 17-4PH, H.D. Kunze (Ed.), *Competitive Advantages by Near-Net-Shape Manufacturing*, DGM Information Shell-chaft, Frankfurt, 1997, pp. 303-308.
- [8] G. Kalin, E.Akdag, S. Ozbey, H.O. Gulsoy, Electrochemical behavior of injection molded gas and water 17-4PH Stainless steel powder, *Advances in Powder Metallurgy and Particulate Materials*, Metal Powder Industries Federation, Princeton 2017, 364-373.
- [9] D. Claudel, M. Sahli, T. Barriere, J-C. Gelin, Influence of particle-size distribution and temperature on the rheological properties of highly concentrated Inconel feedstock alloy 718, *Powder Technol.* 322 (2017) 273–289. <https://doi.org/10.1016/j.powtec.2017.08.049>.
- [10] M.E. Sotomayor, A. Varez, B. Levenfeld, Influence of powder particle size distribution on rheological properties of 316L powder injection molding feedstock, *Powder Technol.* 200 (2010) 30-36. <https://doi.org/10.1016/j.powtec.2010.02.003>.
- [11] M. Seerane, P. Ndlangamandla, R. Machaka, The influence of particle size distribution on the properties of metal injection molded 17-4PH stainless steel, *J. South. Afr. Inst. Min. Metall.* 116 (2016), 935-940. <https://doi.org/10.17159/24119717/2016/v116n10a7>.
- [12] J.M. Contreras, A. Jimenez-Morales, J.M. Torralba, Improvement of rheological properties of Inconel 718 MIM feedstock using tailored particle size distributions, *Powder Metall.* 51 (2008) 103-106. <https://doi.org/10.1179/174329008X313342>.
- [13] B. Hausnerova, B.N. Mukund, D. Sanetnik, Rheological properties of gas and water atomized 17-4PH stainless steel MIM feedstocks: Effect of powder shape and size, *Powder Technol.* 312 (2017) 152-158. <https://doi.org/10.1016/j.powtec.2017.02.023>

- [14] B. Hausnerova, D. Bleyan, V. Kasparkova, V. Pata, Surface adhesion between ceramic injection molding feedstocks and processing tools. *Ceram. Int.* 42 (2016) 460-465. <https://doi.org/10.1016/j.ceramint.2015.08.132>.
- [15] D. Bleyan, B. Hausnerova, P. Svoboda, The development of powder injection moulding binders: A quantification of individual components' interactions. *Powder Technol.* 286 (2015) 84-89. <https://doi.org/10.1016/j.powtec.2015.07.046>.
- [16] R.M. German, Homogeneity effect on feedstock viscosity in Powder Injection Molding, *J. Am. Ceram. Soc.* 77 (1994) 283-285. <https://doi.org/10.1111/j.1151-2916.1994.tb06992.x>
- [17] H. Bohm, S. Blackburn, Effect of mixing procedure on fine alumina paste extrusion, *Br. Ceram. Trans.* 93 (1994) 169-170.
- [18] R.Y. Wu, W.C.J. Wei, Torque evolution and effects on alumina feedstocks prepared by various kneading sequences, *J. Eur. Ceram. Soc.* 20 (2000) 67-75. [https://doi.org/10.1016/S0955-2219\(99\)00061-8](https://doi.org/10.1016/S0955-2219(99)00061-8).
- [19] R. Raman, W. Slike III, R.M. German, C.I. Whitman, Experimental evaluation of the mixing process for the preparation of feedstock for powder injection molding, *Ceram. Eng. Sci. Proc.* 14 (1993) 166-186. <https://doi.org/10.1002/9780470314272.ch12>.
- [20] R. Machaka, P. Ndlangamandla, M. Seerane, Capillary rheological studies of 17-4PH MIM feedstocks prepared using a custom CSIR binder system, *Powder Technol.* 326 (2018) 37-43. <https://doi.org/10.1016/j.powtec.2017.12.051>.
- [21] B. Hausnerova, P. Saha, J. Kubat, Capillary flow of hard-metal carbide powder compounds, *Int. Polym. Proc.* 14 (1999) 254-260. <https://doi.org/10.3139/217.1556> <https://doi.org/>.
- [22] D.F. Heaney, *Handbook of Metal Injection Molding*, first ed., Woodhead Publishing, Philadelphia, 2012.

List of Tables and Figures

Table 1 Characteristics of 17-4PH stainless steel water atomized powders

Table 2 Tailored particle size distributions of 17-4PH water atomized powders

Table 3 Optimum injection molding parameters of 17-4PH water atomized powders

Table 4 Metallurgical parameters of 17-4PH sintered parts after H900 treatment

Figure 1 Complex-shaped MIM component with critical dimensions

Figure 2 SEM micrographs of 66 vol.% feedstocks containing WA_24 (a) and WA_44 (b) powder

Figure 3 Mixing torque as a function of time of 66 vol.% feedstocks containing WA_24, WA_34 and WA_44 powders

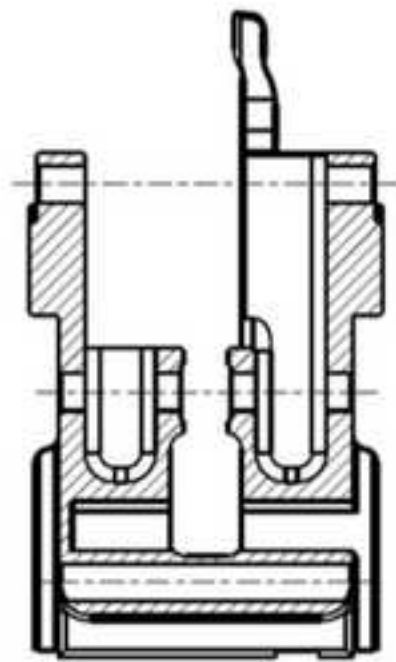
Figure 4 Viscosity as a function of time of 66 vol.% feedstocks containing WA_44 powder (180 °C, 1000 s⁻¹, 3 independent tests)

Figure 5 Viscosity as a function of shear rate of 66 vol.% feedstocks containing WA_24, WA_34 and WA_44 powders (180 °C)

Figure 6 Martensitic microstructure of 17-4PH parts produced from WA_24 (a), WA_34 (b) and WA_44 (c) powders

Figure 7 Dimensional variations indicating a deformation level for WA_24, WA_34 and WA_44 parts at the critical slot dimensions (24±0.12) mm (a) and (20±0.1) mm (b)

Figure 1
[Click here to download high resolution image](#)



SECTION A-A

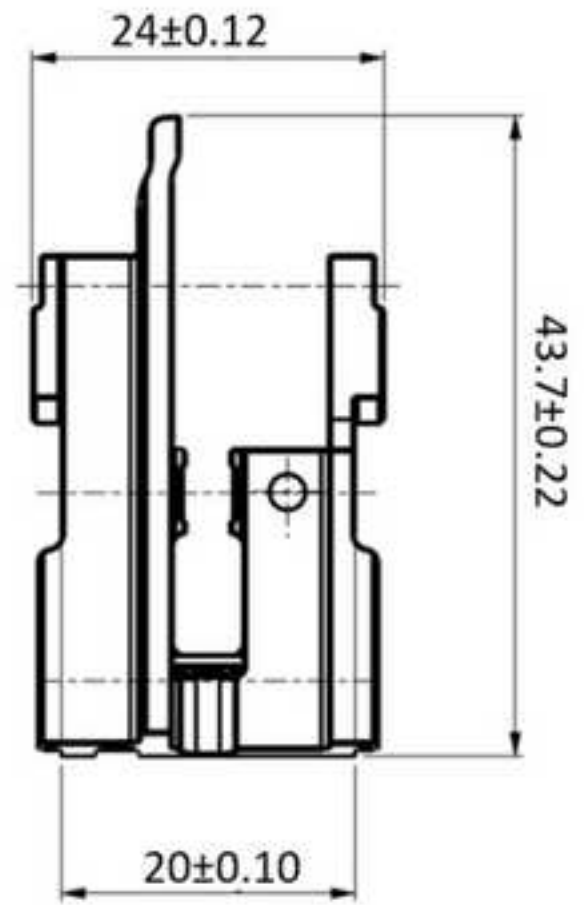
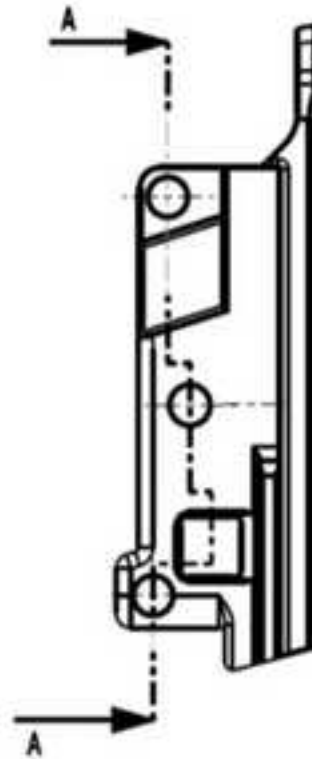


Figure 2a
[Click here to download high resolution image](#)

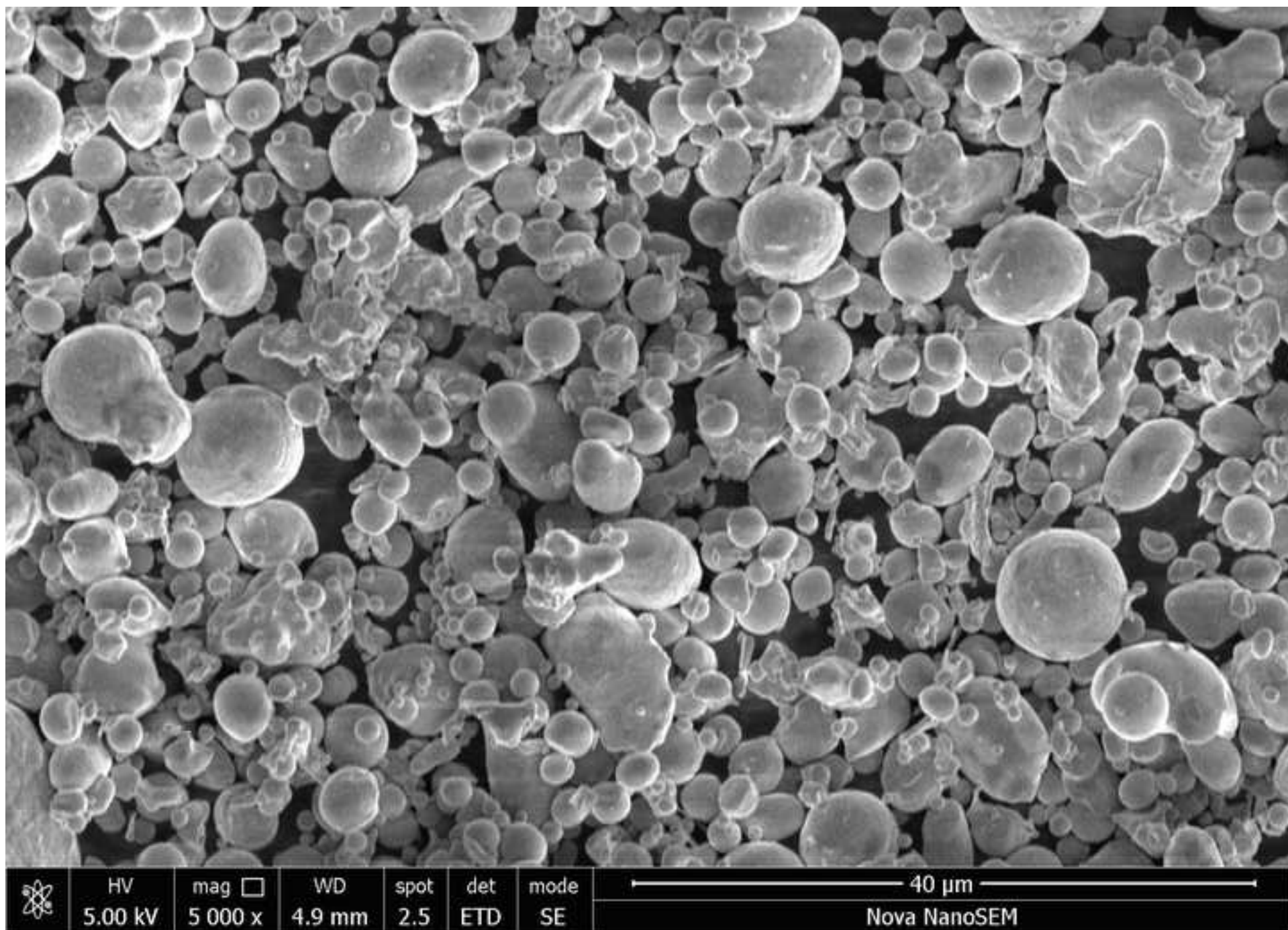
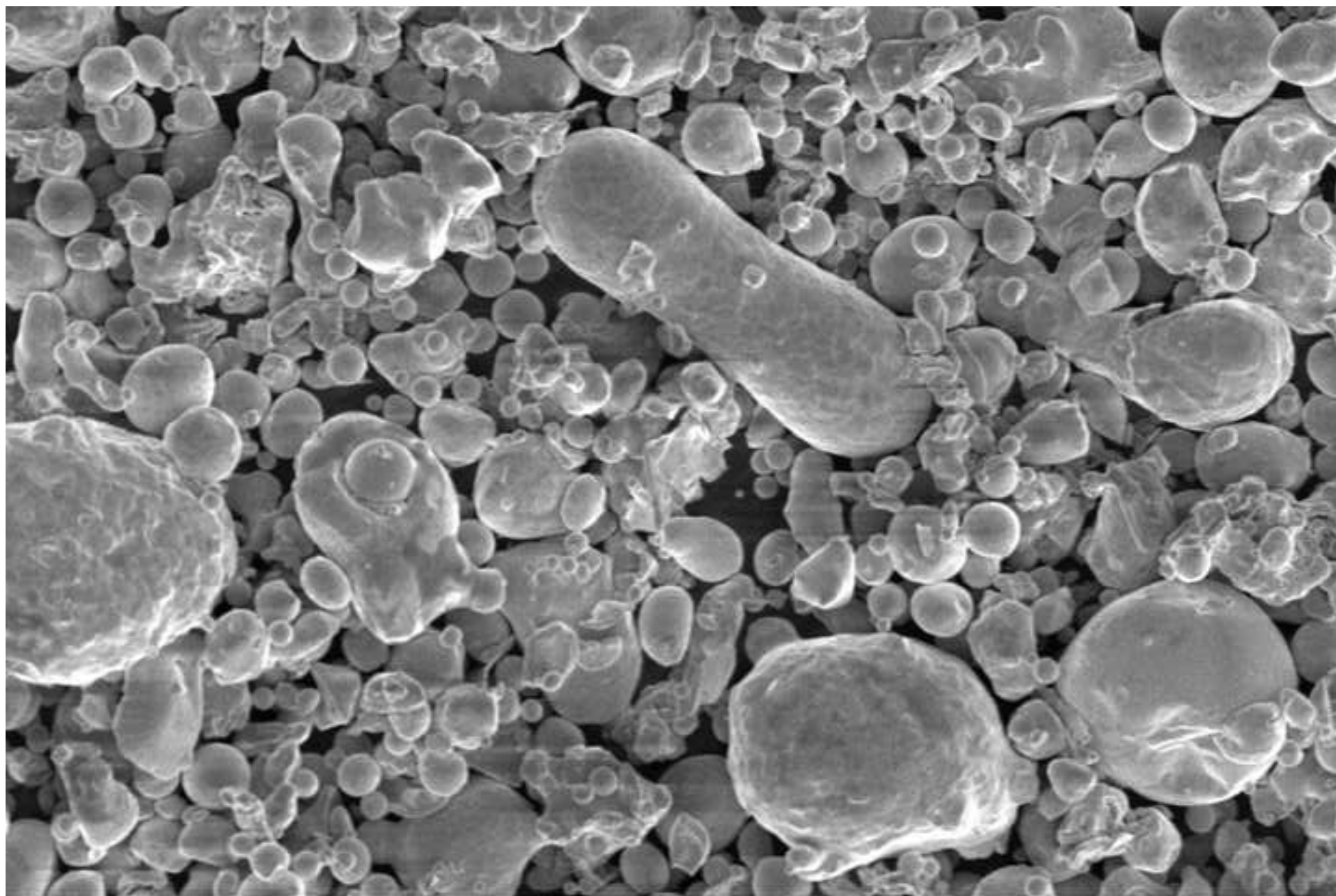


Figure 2b
[Click here to download high resolution image](#)




	HV	mag <input type="checkbox"/>	WD	spot	det	mode	40 μ m	
	5.00 kV	5 000 x	4.9 mm	2.5	ETD	SE	Nova NanoSEM	

Figure 3
[Click here to download high resolution image](#)

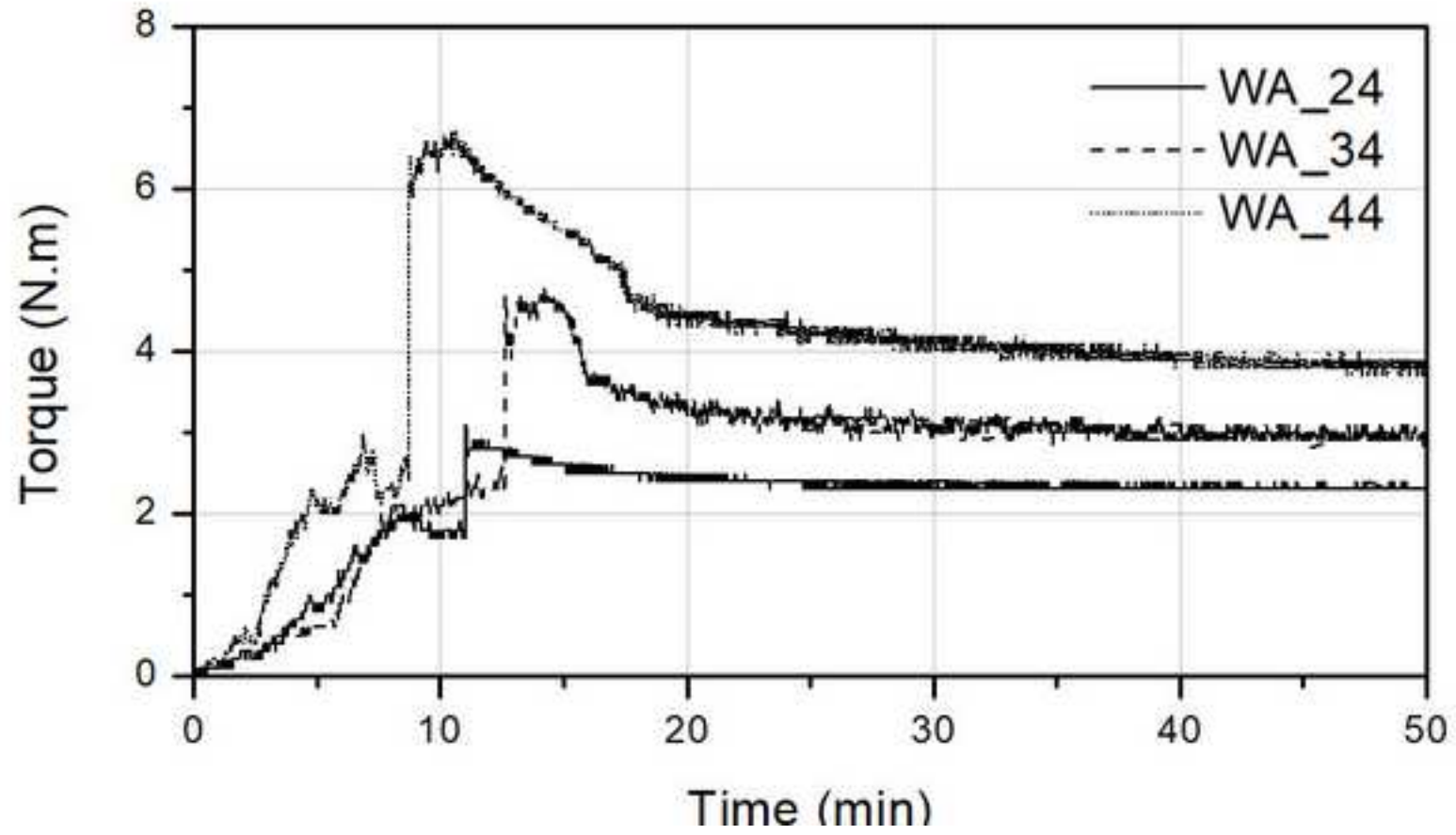


Figure 4
[Click here to download high resolution image](#)

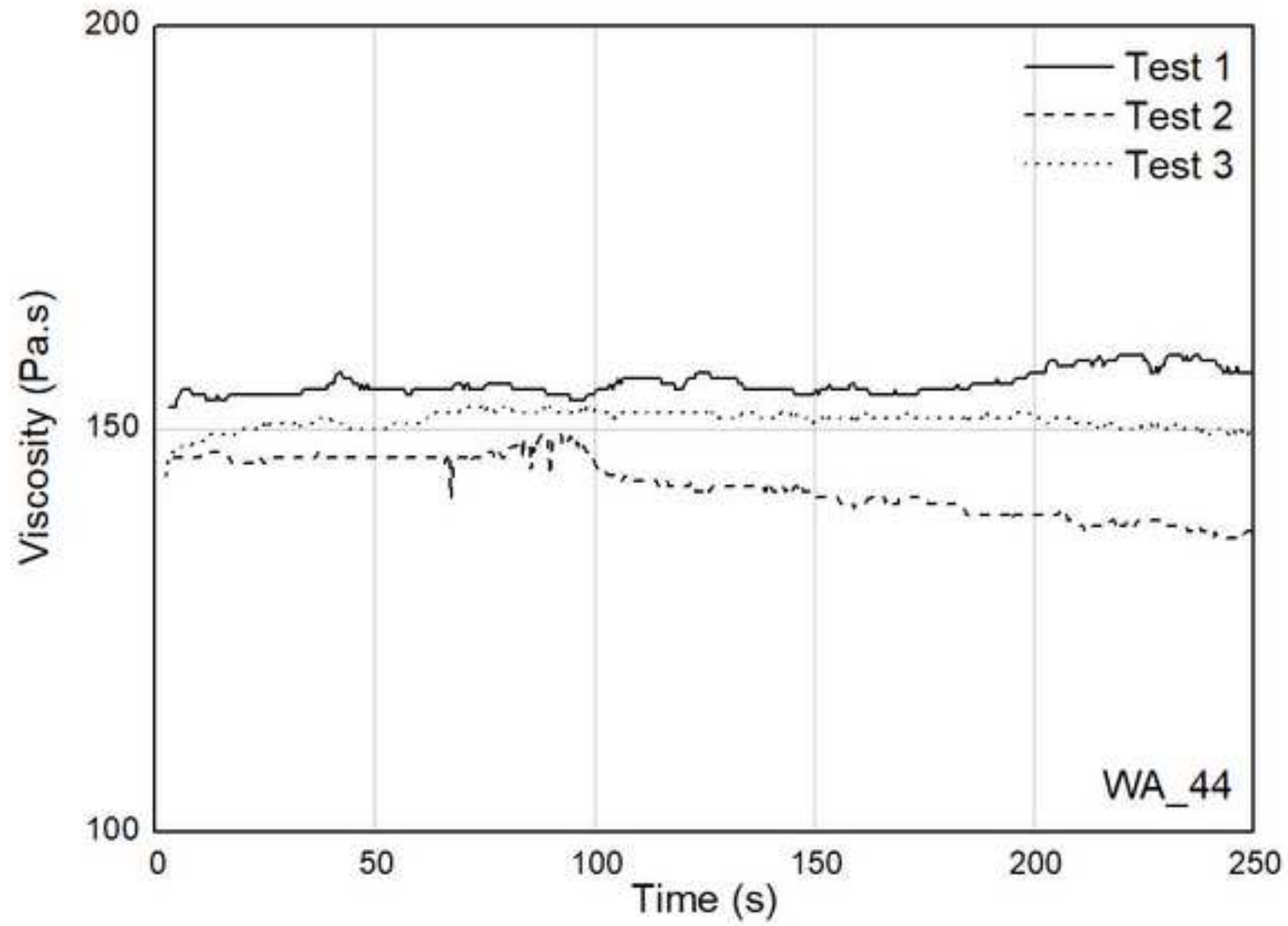


Figure 5
[Click here to download high resolution image](#)

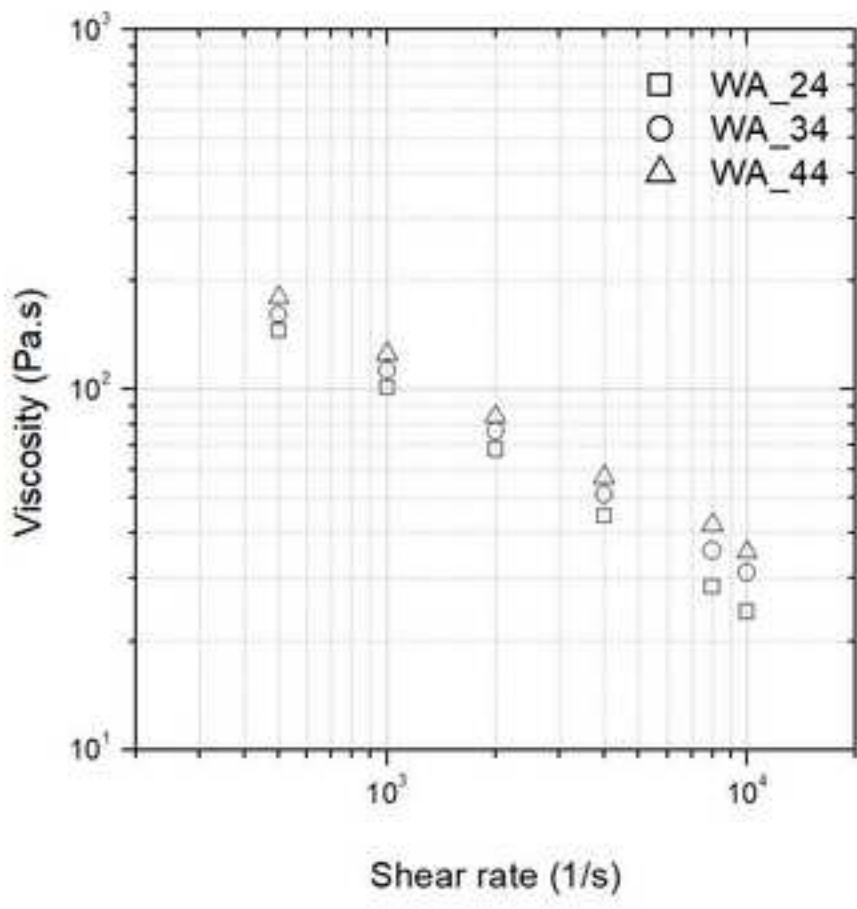


Figure 6a
[Click here to download high resolution image](#)

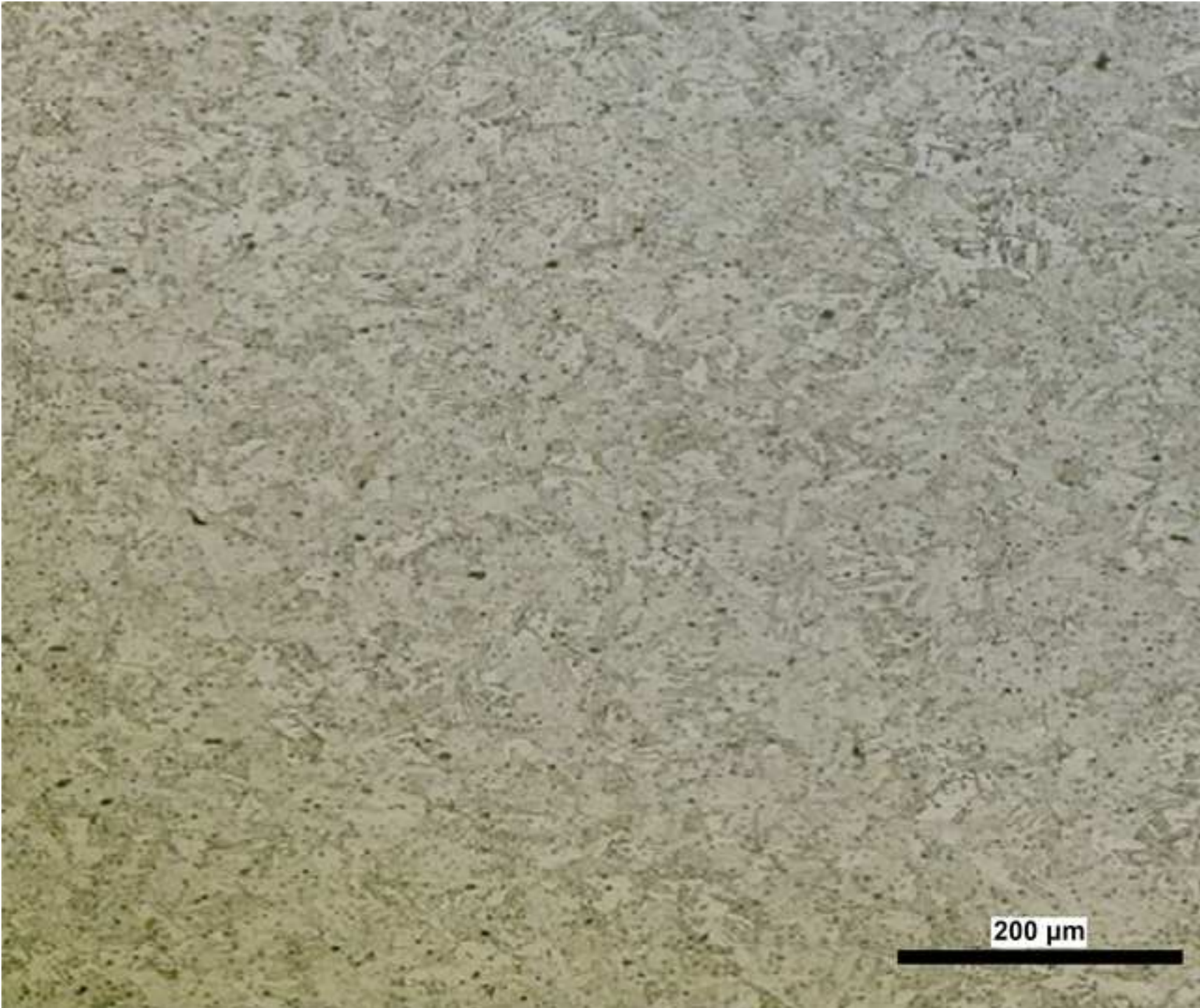


Fig. 6 (a).tif

Figure 6b

[Click here to download high resolution image](#)

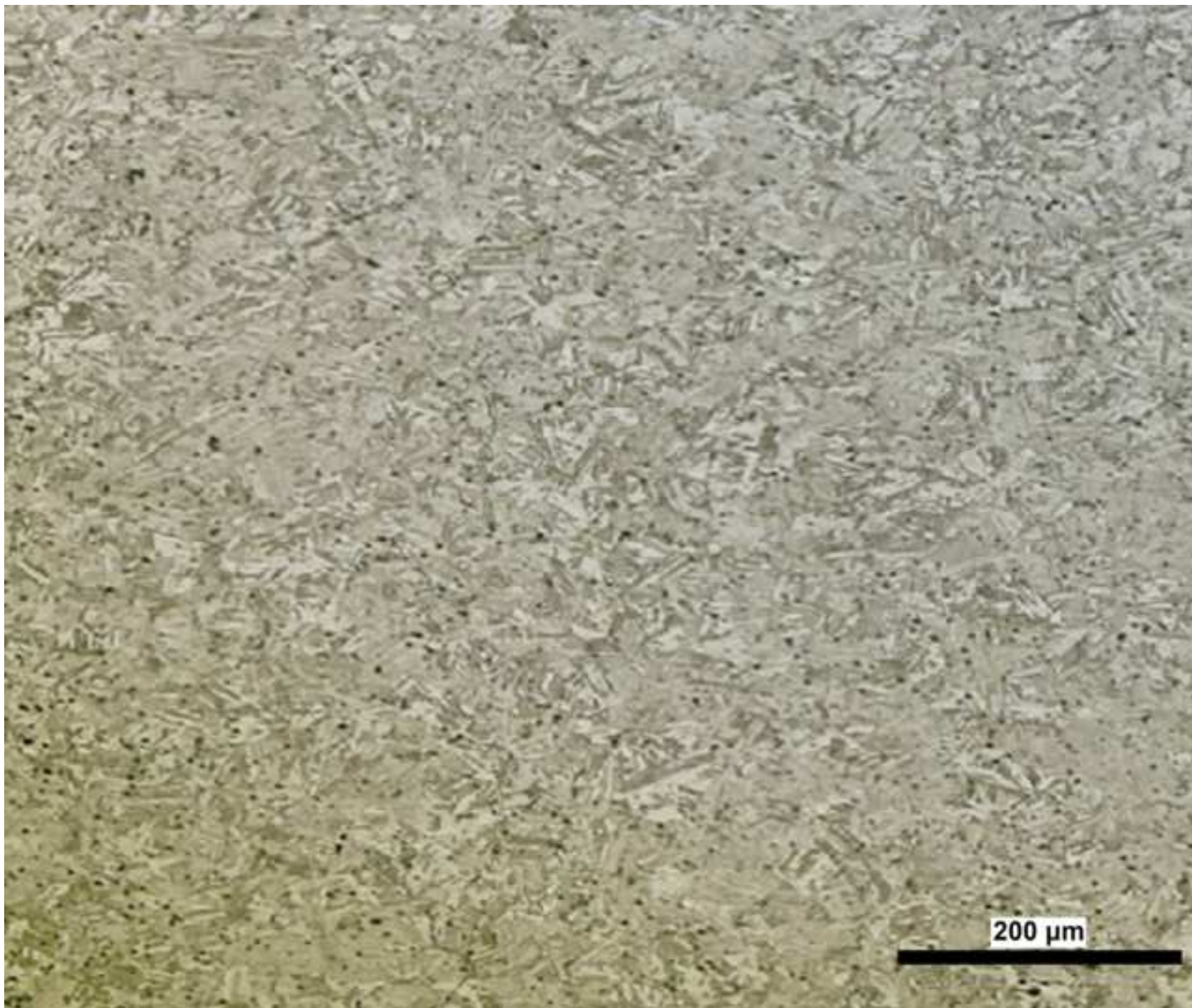


Fig. 6 (b).tif

Figure 6c
[Click here to download high resolution image](#)

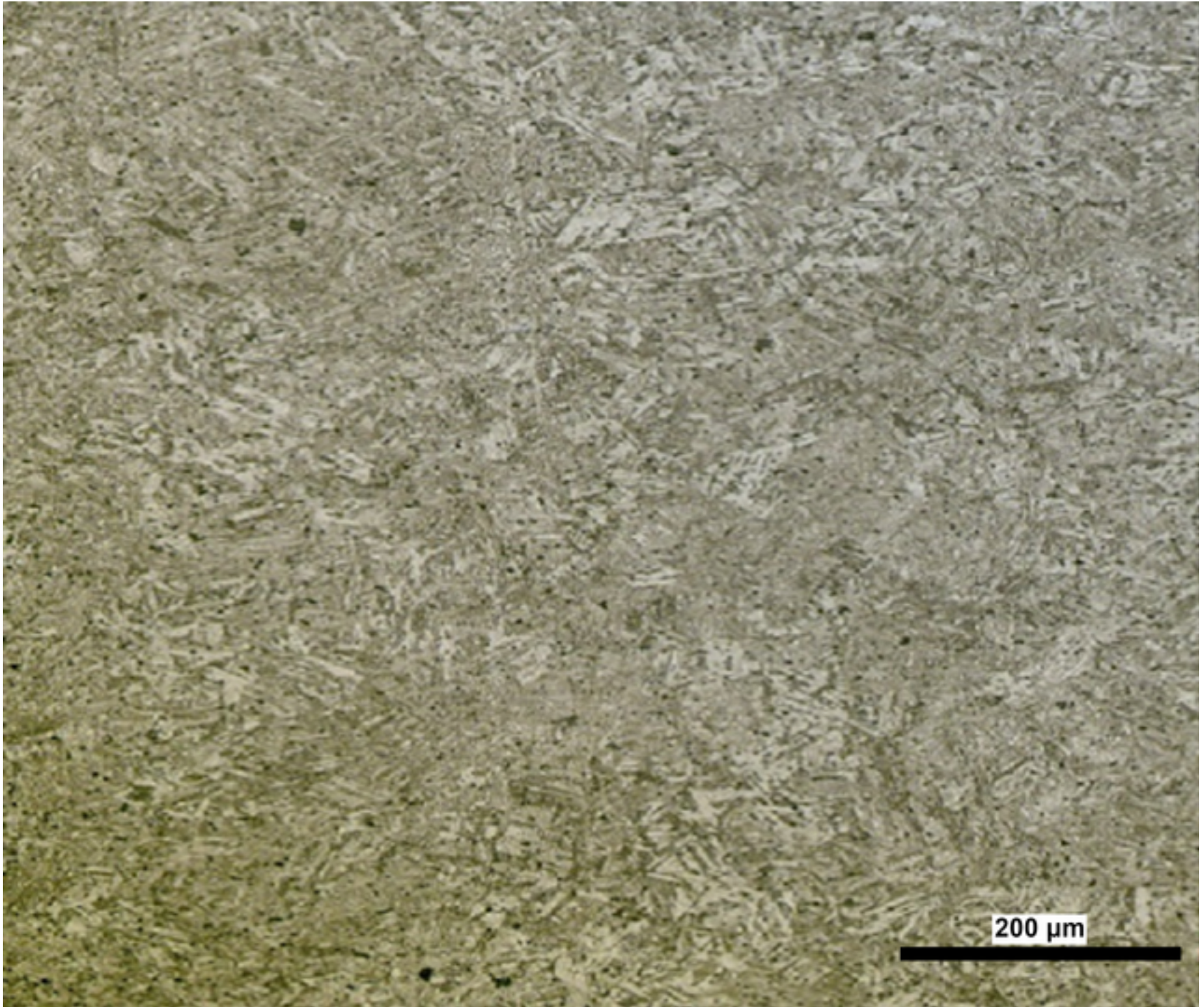


Fig 6 (c).tif

Figure 7a
[Click here to download high resolution image](#)

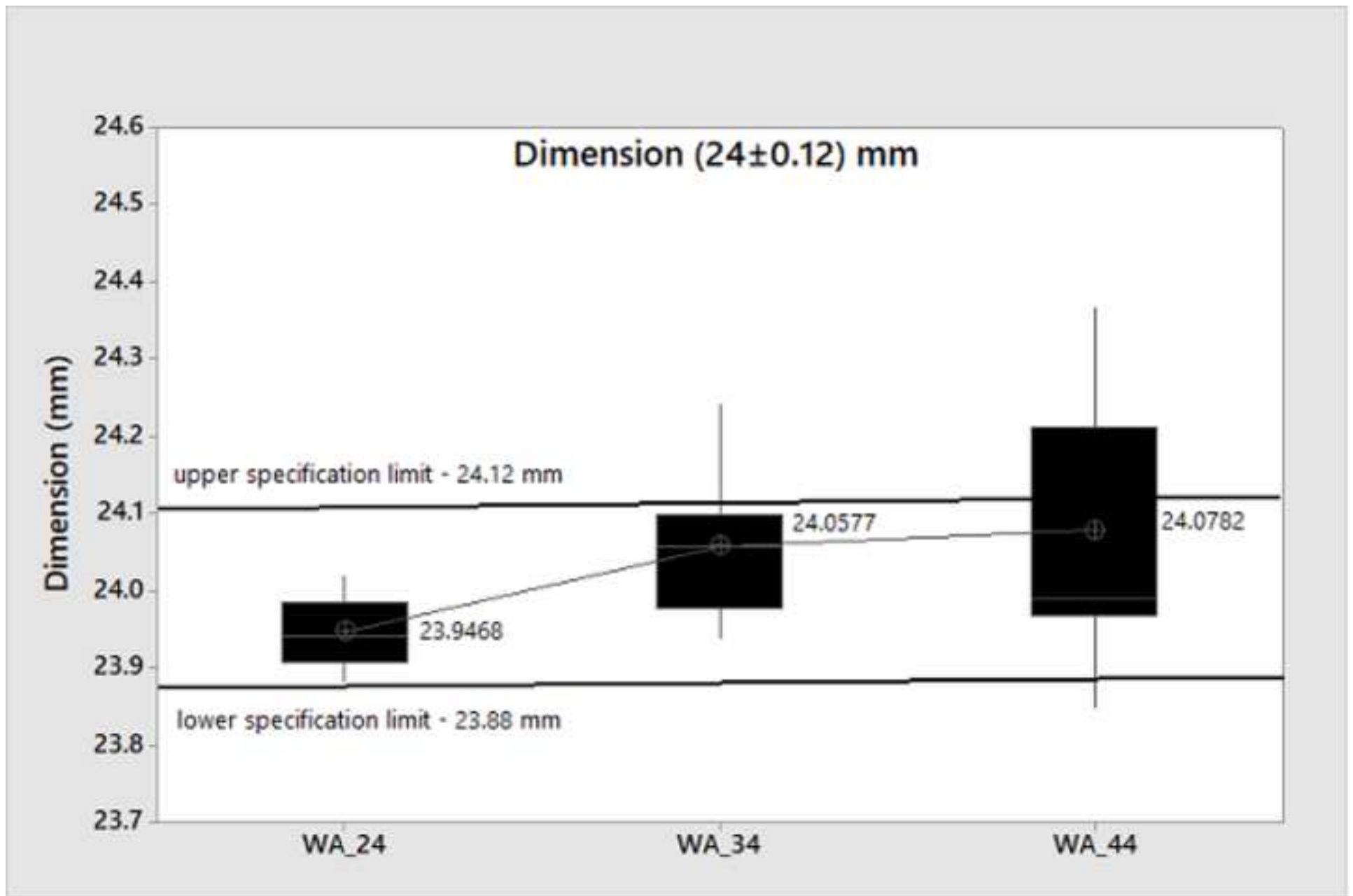


Figure 7b
[Click here to download high resolution image](#)

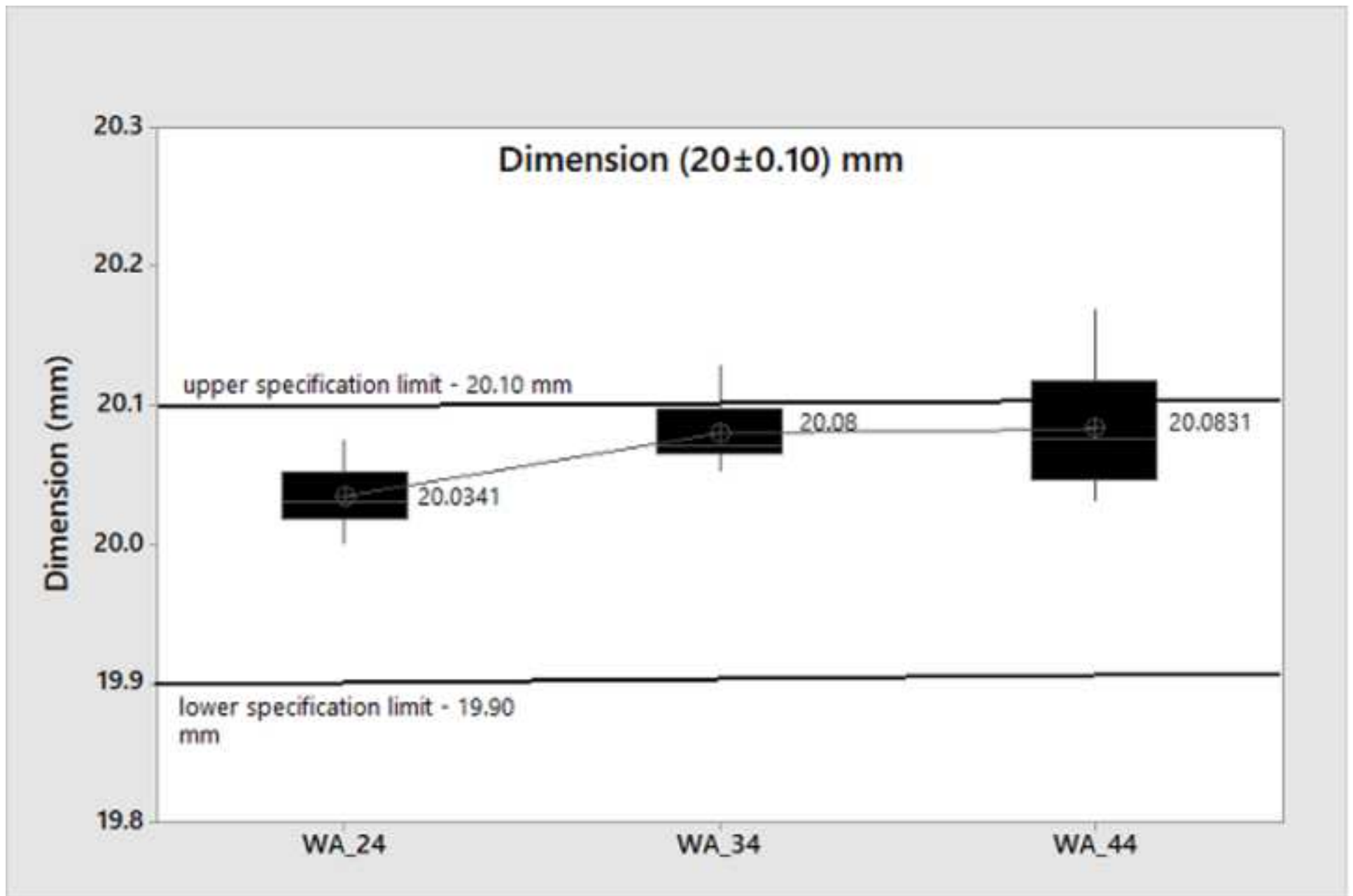


Table 1

Powder	D_{10} (μm)	D_{50} (μm)	D_{90} (μm)	ρ_{pycn} (g/cm^3)	ρ_{tap} (g/cm^3)	S_w (-)
WA_24	3.10	7.64	18.90	7.92	4.15	3.26
WA_34	4.18	8.89	18.40	7.90	4.07	3.92
WA_44	4.34	9.13	19.50	7.90	4.05	3.97

Table 2

Powder	Particle fraction (%)			
	< 5 μm	> 5 μm < 10 μm	> 10 μm < 20 μm	> 20 μm < 35 μm
WA_24	29.93	39.58	23.64	6.85
WA_34	17.45	43.25	33.76	5.54
WA_44	15.19	34.26	43.60	6.95

Table 3

Molding parameter	WA_24	WA_34	WA_44
Nozzle temperature (°C)	180	185	195
Zone temperatures (°C)	180,175,170		
Injection speed (cm ³ /s)	50		
Holding pressure (bar)	800		
Holding time (s)	2.5		
Switch over point (cm ³)	32		
Fill/Cooling time (s)	0.3 /15		
Filling phase amount (%)	60	52	49
Mold temperature (°C)	40		
Change over pressure (bar)	623	758	897

Table 4

Powder	Density (gcm ⁻³)	Carbon content (wt.%)	Hardness (HRC)
WA_24	7.64 - 7.68	0.011 - 0.013	38.8 - 40.6
WA_34	7.60 - 7.65	0.019 - 0.023	38.9 - 39.7
WA_44	7.58 - 7.61	0.021 - 0.028	36.8 - 39.2

Declaration of interests

The authors declare that they have no known competing financial interests or personal relationships that could have appeared to influence the work reported in this paper.

The authors declare the following financial interests/personal relationships which may be considered as potential competing interests:



The image shows a rectangular box containing two handwritten signatures in cursive. The signature on the left is larger and more elaborate, while the signature on the right is smaller and more compact. Both signatures appear to be in black ink on a white background.

Author Contributions:

Berenika Hausnerova: conceptualization; methodology; planning and supervision; writing and revision of the manuscript; funding acquisition

Mukunda Bishmena Naharaj: resources; investigation; formal analysis of the results; writing of the draft of the manuscript

Both authors have read and approved the final manuscript.